

# High modulus hydrogels for ophthalmic and related biomedical applications

Tarnveer S. Bhamra, Brian J. Tighe, Jiffan Li

Biomaterials Research Unit, Chemical Engineering and Applied Chemistry, Aston University, Aston Triangle, Birmingham, B4 7ET, UK

Received 13 April 2018; revised 7 August 2018; accepted 31 August 2018

Published online 00 Month 2018 in Wiley Online Library ([wileyonlinelibrary.com](http://wileyonlinelibrary.com)). DOI: 10.1002/jbm.b.34257

**Abstract:** This paper presents three families of semi-interpenetrating polymer network (SIPN) hydrogels based on an ester-based polyurethane (EBPU) and hydrophilic monomers: *N,N*-dimethylacrylamide (NNDMA), *N*-vinyl pyrrolidone (NVP) and acryloylmorpholine (AMO) as potential materials for keratoprosthesis, orthokeratology and mini-scleral lens application. Hydrogels sheets were synthesized via free-radical polymerization with methods developed in-house. SIPN hydrogels were characterized for their equilibrium water content, mechanical and surface properties. Three families of optically clear SIPN-based hydrogels have been synthesized in the presence of water with >10% of composition attributable to EBPU. Water contents of SIPN materials ranged from 30% to 70%. SIPNs with  $\leq 15\%$  EBPU

of total composition showed little influence to mechanical properties, whereas >15% EBPU contributed significantly to an increase in material stiffness. In the hydrated state, SIPNs with  $\leq 15\%$  EBPU of total composition show little difference in polar component ( $\gamma^p$ ) of surface free energy, whereas for >15% EBPU there is a decrease in  $\gamma^p$ . The EBPU SIPN hydrogels display complementary material properties for keratoprosthesis, orthokeratology, and mini-scleral applications. © 2018 The Authors. *Journal Of Biomedical Materials Research Part B: Applied Biomaterials* Published By Wiley Periodicals, Inc. J Biomed Mater Res B Part B: 00B: 000–000, 2018.

**Key Words:** hydrogel, semi-interpenetrating polymer network, ester-based polyurethane, optical clarity, ophthalmic biomaterial

**How to cite this article:** Bhamra TS, Tighe BJ, Li J. 2018. High modulus hydrogels for ophthalmic and related biomedical applications. *J Biomed Mater Res B Part B*. 2018;00:00:1–9.

## INTRODUCTION

The field of hydrogel-based ophthalmic biomaterials is a long-standing area of application that has, in many cases, led to hydrogel-based studies, which have ultimately been made relevant to a wider range of applications. It is in this context that the present experimental findings are presented.

The human eye exists as a complex self-contained organ and exhibits a set function of providing vision. Vision is provided by the natural light refractive ability of the cornea and final focalization onto the retina via the human crystalline lens. When vision deteriorates, vision-correction devices fashioned from bio-tolerant polymeric materials are required in the contact lens, intraocular lens and artificial corneal tissue format. In this respect, there exists a potential application for a new family of polymer-based materials that lie between compliant hydrogels and rigid lens materials.

The history of the development of ophthalmic biomaterials in the last 50 years has predominantly been in the context of contact lenses. A recent review<sup>1</sup> describes the progressive extension of mechanical properties from stiff

glass and “Plexiglass” poly(methyl methacrylate), PMMA, through to soft hydrogels, in which the desire to mimic the mechanical properties of the surrounding tissue is important. The more successful hydrogel lens materials have lower moduli than those reported for the cornea, which include Young’s modulus values up to 20 MPa.<sup>2–4</sup> It must be noted, however, that these mechanical property measurements relate to various testing and sample presentation configurations and values around 1 MPa are more widely accepted.

There has been a renewed interest in the development of high modulus materials for use in the treatment of diseased corneal tissue and corneal tissue that has been exposed to externally-influenced trauma, in the form of keratoprosthesis (KPro). Developments and applications of material designs in KPro have been well documented,<sup>5–7</sup> though few recent novel material-combinations have been described.<sup>8–10</sup> The use of the Boston KPro<sup>11,12</sup> and the osteo-odonto-keratoprosthesis<sup>13</sup> still dominate clinical application in the field.

Rigid gas-permeable (RGP) lens materials<sup>14</sup> have seen a resurgence in the application of orthokeratology (OrthoK),

**Correspondence:** Tarnveer S. Bhamra; e-mail: [biostuff@aston.ac.uk](mailto:biostuff@aston.ac.uk)

This is an open access article under the terms of the Creative Commons Attribution-NonCommercial-NoDerivs License, which permits use and distribution in any medium, provided the original work is properly cited, the use is non-commercial and no modifications or adaptations are made.

whereby overnight wear of these materials in the contact lens format can temporarily reduce refractive errors for vision improvement.<sup>15-18</sup> Use of RGP materials has also been reported in the design of scleral and mini-scleral lenses,<sup>19,20</sup> for use as a post-surgical ocular bandage<sup>21</sup> and with new silicone hydrogel (SiHy)-based materials<sup>22</sup> currently under investigation. Additionally, combinations of RGP and soft hydrogel materials in the form of "piggyback" lenses<sup>23</sup> are used in the correction of keratoconus.<sup>24</sup>

Design of a material to be a suitable candidate for KPro, OrthoK, and mini-scleral lenses requires fulfillment of a set of criteria that complements the ocular environment. These criteria include:

- Optical clarity
- Dimensional stability for ease of lens-handleability
- Sufficient durability and flexibility to withstand the stresses applied when surgically sutured into the eye for KPro
- Susceptibility to cellular integration of KPro implant
- High modulus to re-shape corneal surface overnight in the case of OrthoK
- Sufficient oxygen permeability to ensure minimal disruption of any aerobic biological processes, that occur at the external and intra-vascular ocular environment
- Sufficient surface wettability to support tear film spreading
- Bio-tolerance to ocular fluids at the material surface-tear film interface
- Availability and ease of manufacture with existing technology

Though there exists a significant cross-over for the combinations of material properties required for KPro, OrthoK, and mini-scleral lenses, a trade-off in material properties displayed by the hydrogels presented herein, compared to the ideal material requirements in each respective application, is inevitable. Oxygen permeability is an important aspect of any ophthalmic material and although this property is not considered directly here, it is a direct consequence of the ability of hydrogel materials to imbibe water. The equilibrium water content (EWC) of a non-silicone hydrogel is known to govern its oxygen permeability.<sup>25</sup>

Conventional co-polymeric hydrogels can achieve water contents similar to those reported for ocular tissue,<sup>26</sup> however these materials possess poor mechanical properties at higher water contents. Hydrogel networks can be reinforced to obtain improved mechanical properties with water contents akin to those of conventional hydrogels, through the use of interpenetrating and semi-interpenetrating polymer networks (SIPNs).<sup>27,28</sup> SIPNs are a combination of one linear polymer and one cross-linked polymer network. An ester-based polyurethane (EBPU) is used as an interpenetrant to produce SIPNs, exploiting the excellent mechanical properties and good biocompatibility of these materials.<sup>28,29</sup>

The long-term stability of materials in a hydrated environment, as indicated by a resistance to hydrolytic degradation, is important for many ophthalmic applications.

Resistance to hydrolytic degradation can be provided by amide-based monomers in interpenetrating hydrogel networks.<sup>30</sup> In this study, we assess the long-term stability of EBPU SIPNs fabricated from amide-containing monomers, in a hydrated environment.

One very significant aspect of the novelty of the SIPN hydrogel materials described here as candidates for challenging ophthalmic and related applications, in which high modulus combined with moderate (40–60%) EWC is required, is that the thermodynamic difficulties involved in the miscibility of polymer components<sup>28</sup> have been overcome to achieve families of optically clear hydrogel SIPNs. Typical publications describing the properties of hydrogel SIPN materials report optical clarity with only  $\leq 5\%$  of the interpenetrant polymer.<sup>31,32</sup> The liquid amide-containing monomers *N,N*-dimethylacrylamide (NNDMA), *N*-vinyl pyrrolidone (NVP), and acryloylmorpholine (AMO) were found to have extended solubility and compatibility ranges with EBPU. This enabled three families of optically clear EBPU-based hydrogel SIPNs to be prepared. This article presents the water-binding characteristics, mechanical and surface properties of these materials.

## MATERIALS AND METHODS

### Materials

Acryloylmorpholine, *N*-vinyl pyrrolidone, and methyl methacrylate were purchased from Vista Optics (Widnes, UK). *N,N*-dimethylacrylamide (NNDMA) and azo-bis-isobutyronitrile (AZBN) were purchased from Sigma-Aldrich (Gillingham, UK). Tetrahydrofurfuryl methacrylate (THFMA) was from Polysciences (Warrington, PA). EBPU was obtained from B.F. Goodrich (Brecksville, OH). Ethylene glycol dimethacrylate (EGDMA) was supplied by Sigma-Aldrich (Gillingham, UK). The monomers were purified by reduced pressure distillation and stored in a refrigerator before use.<sup>33</sup>

### Membrane polymerization

Two glass plates (15 × 10 cm) were each covered with a sheet of poly(ethylene terephthalate), (Melinex) secured by a spray-mount, and surface cleaned with acetone. The plates were placed together with two polyethylene gaskets, each 0.2 mm thick, separating the Melinex sheets (cavity 5 × 9 cm). The whole mold was held together by spring clips and the monomer mixture was injected into the mold cavity using a G22 syringe needle and syringe. The standard monomer mixture was made up to 5.0 g in mass, with 1.0% w/w crosslinker EGDMA and 0.5% w/w initiator AZBN. Mixture was degassed with nitrogen for 10 min prior to injection. The mixture was injected into the mold via syringe and needle. The injected mold was then incubated at 60°C for 3 days to allow polymerization, followed by a 3-h post-cure at 90°C. The membrane was then removed from the mold and placed in distilled water to hydrate and reach equilibrium. Hydration was allowed to proceed for at least 1 week and water was replaced daily. Complete hydration and polymerization achieved based on previous work within the group, see discussion for details.

### Equilibrium water content measurement

The EWC, was measured from weight differences. Samples of the hydrated membrane sheet were cut with a size seven cork-borer, and excess surface water was removed with filter paper. The weighed hydrated samples were then dehydrated in an 800 W microwave for 15 min at high power. Samples were reweighed and the EWC was calculated with Eq. (1). Measurements were triplicated and an average value determined.

$$\text{EWC (\%)} = \frac{\text{Weight of water in the gel}}{\text{Total weight of the hydrated gel}} \times 100\% \quad (1)$$

### Freezing water content measurement

Differential Scanning Calorimetry (DSC) was used to determine the percentage of the freezing water content (FWC) present in a hydrogel sample. Thermograms were obtained using a Perkin-Elmer DSC-7, in conjunction with a 7500 professional computer and liquid nitrogen cooling accessory. A hydrogel sample was cut from the hydrated membrane using a size one cork-borer and excess surface water was removed with filter paper. The small weighed samples (4.0–7.0 mg) were sealed in aluminum pans and the following thermal change steps were applied to each sample respectively: cool from 20°C to –70°C at 100 °C/min, hold for 5 min at –70°C, heat from –70°C to –25°C at 20°C/min, heat from –25°C to 20°C at 10 °C/min. From the thermograms produced, the area under the endothermic peaks was converted to the weight of freezing water in the sample *via* the heat of fusion of pure water. Measurements were triplicated and an average value determined.

### Mechanical property measurements

The tensile properties of the fully hydrated hydrogels were investigated using a Hounsfield Hti tensometer, interfaced to an IBM 55SX computer. The tensometer was fitted with a 10 N load cell. Dumbbell-shaped samples of width 3.3 mm were cut from the hydrogels and sample thickness was measured with a 10 mm diameter probe micrometer. Tests were carried out using a crosshead speed of 20 mm min<sup>-1</sup>. For the duration of the test, the sample was hydrated by an application of a fine mist of water from an atomizer onto its surface. Upon completion, the software calculated the tensile modulus (TM), tensile strength (TS), and elongation to break (ETB). Measurements were triplicated and an average value determined.

### Surface properties measurement

The surface energies of hydrogels were calculated under two sets of conditions:

- A. In the hydrated state using the Hamilton and captive air bubble techniques (restricted to polar contribution to total surface free energy only).
- B. In the dehydrated state using the sessile drop technique.

Contact angles were measured using a contact angle goniometer (Digidrop GBX) with an inbuilt CCD video camera. The computer controlled stage was used to ensure that the droplet was placed on the material with a reproducible volume. The polar ( $\gamma^p$ ), dispersive ( $\gamma^d$ ), and total ( $\gamma^t$ ) surface free energies were (then) calculated. Measurements were triplicated and an average value determined.

**Hamilton's method.** Discs were cut from the hydrated hydrogel membrane using a size seven cork-borer. Excess surface water was removed from the sample with filter paper. The sample was fixed to an electron microscope stub using super glue, inverted and suspended in an optical cell which was filled with distilled water. A drop of *N*-octane was placed on the surface of the sample using a curved G25 syringe needle.

**Captive air bubble technique.** Samples were cut and mounted as described above for Hamilton's method. Air bubbles were then released onto the surface using a specially curved syringe G25 needle.

**Sessile drop technique.** Samples were cut out using a size seven cork-borer and were dehydrated to constant weight in a microwave oven for approx. 15 min. Samples were kept flat by dehydrating between two blocks of poly(tetrafluoroethylene), PTFE. They were placed on a microscope slide located on the sample stage of the contact angle goniometer.

## RESULTS

### Water content

The EWC of MMA-based copolymers synthesized in this work varied from 34.7% to 84.5% and that of the SIPNs varied from 30.7% to 70.3% (Fig. 1). Figure 2 highlights that when EWC of the SIPN-based hydrogels increased, there was a simultaneous increment in the FWC. Additionally, the FWC of each SIPN did not change significantly when the proportion of hydrophilic monomers was increased.

### Mechanical properties

The SIPN hydrogels and their equivalent MMA-based copolymers synthesized in this work possess a wide range of mechanical properties, as shown in Tables I and II, respectively. At EBPU contents of ≤15.0% (by weight), the TM, TS, and ETB of the three SIPN materials did not change significantly when EBPU content was increased. However, at EBPU contents of >15.0% the TM and TS were amplified when the proportion of EBPU is increased.

### Surface properties

As shown in Table I, a small change exists in the hydrated  $\gamma^p$  as EBPU content was increased from 10.0% to 15.0% (by weight), however note as  $\gamma^p$  decreases when EBPU content was increased to 16.8%. When EBPU content was increased to ≥16.8% there was no significant effect on  $\gamma^p$ . Note the narrow distribution of the data points, dehydrated

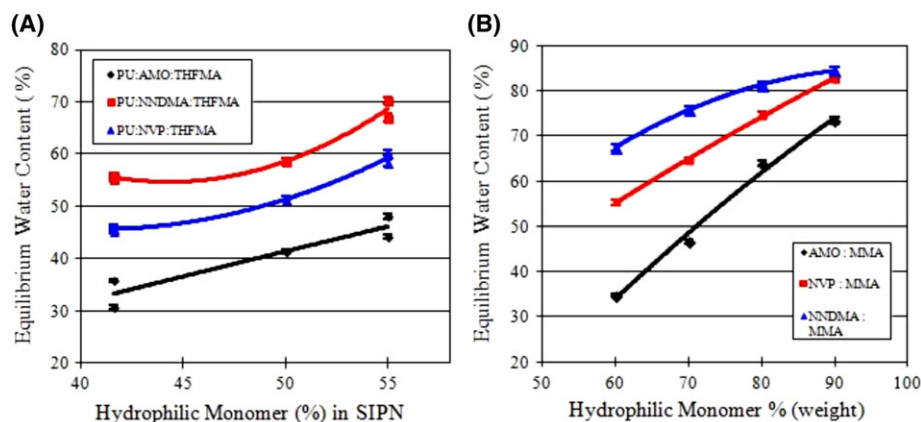


**FIGURE 1.** The equilibrium water content of SIPNs (A) and simple MMA copolymers (B). (Data from Tables I and II – for ease of visual presentation the error bars are not shown). [AMO; acryloylmorpholine, EWC; equilibrium water content, MMA; methyl methacrylate, NNDMA; *N,N*-dimethylacrylamide, NVP; *N*-vinyl pyrrolidone, PU; ester-based polyurethane, and SIPN; semi-interpenetrating network].

$\gamma^t$  varied from 38.1 to 47.2  $\text{mN m}^{-1}$  and hydrated  $\gamma^p$  varied from 22.9–32.2  $\text{mN m}^{-1}$ .

## DISCUSSION

The underlying polymerization methodologies (time, temperature and initiator) are well-established in the contact lens field for the preparation of xerogels that are subsequently lathed into prescription hydrogel contact lenses.<sup>25</sup> In earlier membrane polymerization studies involving methacrylate, vinyl amide, and acrylamido monomers, levels of residual monomer and cross-linking agent in the hydration medium were determined on a daily basis using gas chromatography. The polymerization and hydration protocol used produce

>95.0% monomer conversion and undetectable residual monomer.<sup>34–37</sup> The techniques for measurement of EWC<sup>34–36,38</sup> and surface properties<sup>39</sup> have also been well documented.

The EWC is the single most important property of a hydrogel because it governs the gas-permeability of membranes, mechanical properties, surface properties, and the resultant behavior at biological interfaces. Water plays an important role in determining the biocompatibility of synthetic materials. Materials with high water contents possess similarities with normal tissues found in the biological environment (body). They also ensure a low interfacial tension with blood which reduces protein adsorption and cell adhesion. This advantage has been known as an essential

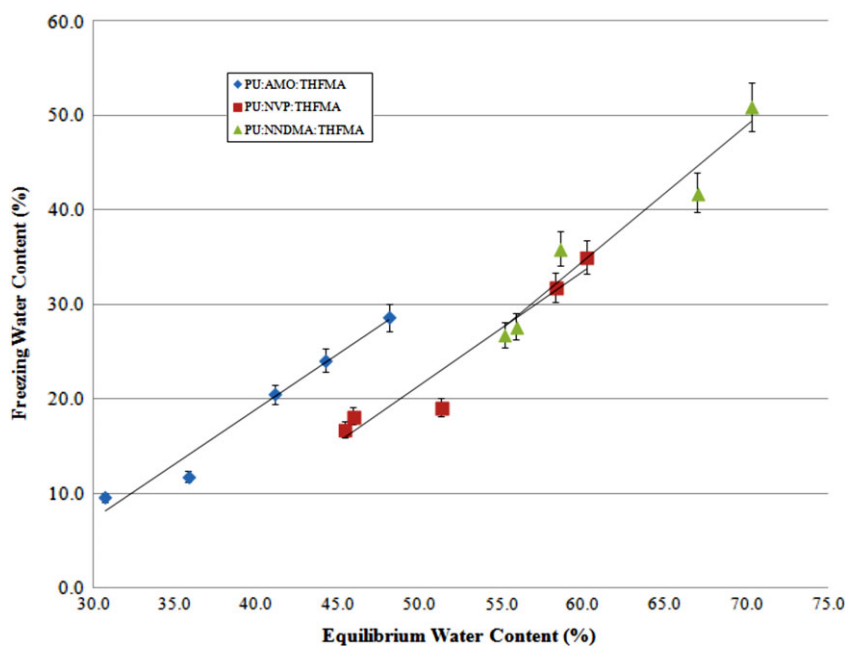


**FIGURE 2.** Equilibrium water content versus freezing water content for clear SIPNs (Data from Table I – horizontal error bars not shown for ease of visual presentation). [AMO; acryloylmorpholine, MMA; methyl methacrylate, NNDMA; *N,N*-dimethylacrylamide, NVP; *N*-vinyl pyrrolidone, PU; ester-based polyurethane, SIPN; semi-interpenetrating network].

TABLE I. Material Property Measurements for Clear SIPNs

Sample no.	Monomer content (%) <sup>a</sup>					Surface free energy (mN m <sup>-1</sup> )														
	EBPU	THFMA	AMO	NVP	NNDMA	Tensile properties					Dehydrated					Hydrated				
						Tensile modulus (MPa)	Tensile strength (MPa)	Elongation to break (%)	Polar ( $\gamma^p$ )	Dispersive ( $\gamma^d$ )	Total ( $\gamma^t$ )	Polar ( $\gamma^p$ )	Dispersive ( $\gamma^d$ )	Total ( $\gamma^t$ )	Polar ( $\gamma^p$ )	Dispersive ( $\gamma^d$ )	Total ( $\gamma^t$ )			
S1	10.0	35.0	55.0	-	-	44.2 ± 2.2	24.1 ± 1.2	24.1 ± 1.2	0.9 ± 0.2	85.0 ± 34.0	5.7 ± 0.3	39.5 ± 2.0	45.2 ± 2.3	30.4 ± 1.5						
S2	-	-	-	55.0	-	60.2 ± 3.0	35.0 ± 1.8	35.0 ± 1.8	0.8 ± 0.2	102.7 ± 41.1	2.0 ± 0.1	41.3 ± 2.1	43.3 ± 2.2	32.2 ± 1.6						
S3	-	-	-	-	55.0	70.3 ± 3.5	50.9 ± 2.5	50.9 ± 2.5	0.1 ± 0.0	73.4 ± 29.4	0.4 ± 0.0	44.4 ± 2.2	44.8 ± 2.2	31.3 ± 1.6						
S4	15.0	30.0	55.0	-	-	48.1 ± 2.4	28.6 ± 1.4	28.6 ± 1.4	1.1 ± 0.2	87.0 ± 34.8	9.7 ± 0.5	35.5 ± 1.8	45.2 ± 2.3	30.4 ± 1.5						
S5	-	-	-	55.0	-	58.3 ± 2.9	31.8 ± 1.6	31.8 ± 1.6	1.7 ± 0.3	35.0 ± 14.0	0.9 ± 0.0	40.4 ± 2.0	41.3 ± 2.1	30.7 ± 1.5						
S6	-	-	-	-	55.0	67.0 ± 3.4	41.8 ± 2.1	41.8 ± 2.1	0.7 ± 0.1	62.0 ± 24.8	2.3 ± 0.1	41.1 ± 2.1	43.4 ± 2.2	31.0 ± 1.6						
S7	16.8	41.6	41.6	-	-	30.7 ± 1.5	9.6 ± 0.5	9.6 ± 0.5	4.5 ± 0.9	102.8 ± 41.1	2.3 ± 0.1	41.1 ± 2.1	43.4 ± 2.2	23.5 ± 1.2						
S8	-	-	-	41.6	-	45.9 ± 2.3	18.2 ± 0.9	18.2 ± 0.9	3.5 ± 0.7	82.3 ± 32.9	9.5 ± 0.5	43.9 ± 2.2	-	24.1 ± 1.2						
S9	-	-	-	-	41.6	55.9 ± 2.8	27.7 ± 1.4	27.7 ± 1.4	0.4 ± 0.1	43.4 ± 17.4	3.3 ± 0.2	40.7 ± 2.0	44.0 ± 2.2	23.5 ± 1.2						
S10	20.0	30.0	50.0	-	-	41.4 ± 2.1	20.5 ± 1.0	20.5 ± 1.0	1.7 ± 0.4	82.1 ± 32.8	1.9 ± 0.1	40.1 ± 2.0	42.0 ± 2.1	22.9 ± 1.1						
S11	-	-	-	50.0	-	51.3 ± 2.6	19.1 ± 1.0	19.1 ± 1.0	1.7 ± 0.3	22.5 ± 9.0	2.8 ± 0.1	39.7 ± 2.0	42.5 ± 2.1	-						
S12	-	-	-	-	50.0	58.6 ± 2.9	35.9 ± 1.8	35.9 ± 1.8	0.4 ± 0.1	39.7 ± 15.9	0.4 ± 0.0	46.8 ± 2.3	47.2 ± 2.4	-						
S13	21.8	36.6	41.6	-	-	35.8 ± 1.8	11.8 ± 0.6	11.8 ± 0.6	2.2 ± 0.4	79.5 ± 31.8	5.3 ± 0.3	33.3 ± 1.7	38.6 ± 1.9	24.1 ± 1.2						
S14	-	-	-	41.6	-	45.4 ± 2.3	16.8 ± 0.8	16.8 ± 0.8	1.7 ± 0.3	30.0 ± 12.0	3.5 ± 0.2	42.8 ± 2.1	46.3 ± 2.3	24.7 ± 1.2						
S15	-	-	-	-	41.6	55.2 ± 3.5	26.8 ± 1.3	26.8 ± 1.3	0.6 ± 0.1	37.5 ± 15.0	7.0 ± 0.4	34.9 ± 1.7	41.9 ± 2.1	25.2 ± 1.3						

<sup>a</sup>AMO; acryloylmorpholine, EBPU; ester-based polyurethane, NNDMA; N,N-dimethylacrylamide, NVP; N-vinyl pyrrolidone, THFMA; tetrahydrofurfuryl methacrylate.

<sup>b</sup>EWC; equilibrium water content.

<sup>c</sup>FWC; freezing water content.

**TABLE II. Material Property Measurements for Simple MMA-Based Copolymers**

Sample no.	Monomer content (%) <sup>a</sup>					Tensile properties		
	MMA	AMO	NVP	NNDMA	EWC <sup>b</sup> (%)	Tensile modulus (MPa)	Tensile strength (MPa)	Elongation to break (%)
C1	10	90.0	–	–	73.4 ± 3.7	0.2 ± 0.0	0.1 ± 0.0	70.0 ± 28.0
C2	–	–	90.0	–	82.8 ± 4.1	0.2 ± 0.0	0.0 ± 0.0	27.0 ± 10.8
C3	–	–	–	90.0	84.5 ± 4.2	0.2 ± 0.0	0.2 ± 0.0	84.0 ± 33.6
C4	20	80.0	–	–	63.9 ± 3.2	0.2 ± 0.0	0.1 ± 0.0	83.0 ± 33.2
C5	–	–	80.0	–	74.6 ± 3.7	0.2 ± 0.0	0.2 ± 0.0	90.0 ± 36.0
C6	–	–	–	80.0	81.3 ± 4.1	0.2 ± 0.0	0.1 ± 0.0	77.0 ± 30.8
C7	30	70.0	–	–	46.6 ± 2.3	0.3 ± 0.0	0.3 ± 0.1	140.0 ± 56.0
C8	–	–	70.0	–	64.6 ± 3.2	0.5 ± 0.1	1.1 ± 0.2	264.0 ± 105.6
C9	–	–	–	70.0	75.9 ± 3.8	0.2 ± 0.0	0.1 ± 0.0	61.0 ± 24.4
C10	40	60.0	–	–	34.7 ± 1.7	8.1 ± 0.8	1.2 ± 0.2	299.0 ± 119.6
C11	–	–	60.0	–	55.3 ± 2.8	2.1 ± 0.2	2.7 ± 0.5	158.0 ± 63.2
C12	–	–	–	60.0	67.5 ± 3.4	0.3 ± 0.0	0.2 ± 0.0	84.0 ± 33.6

<sup>a</sup>AMO; acryloylmorpholine, MMA; methyl methacrylate, NNDMA; *N,N*-dimethylacrylamide, NVP; *N*-vinyl pyrrolidone.

<sup>b</sup>EWC; equilibrium water content.

requisite for the utilization of synthetic material in contact with physiological fluids such as blood.

Materials designed for ophthalmic applications should allow the ready diffusion of macromolecular nutrients to maintain the epithelium and keratocytes. The function is mainly executed by water in the hydrogels. Thus the water content is an important factor that should be considered when developing potential ophthalmic materials. The SIPNs produced have similar water contents to conventional copolymer hydrogels. Poly(2-hydroxyethyl methacrylate), PHEMA is known to have approximately 40.0% EWC and cannot be increased. Higher water content materials than shown here are achievable by an increase in the proportion of the hydrophilic monomer (NNDMA, NVP, and AMO).

Water exists in a continuum of states between two extremes in hydrogels, ranging from freezing, or “free”

water, which is water that does not interact with the polymer matrix, to non-freezing, or “bound” water, which is water that has direct hydrogen bonding with polar groups of the polymer matrix or strongly interacts with ionic residues of the matrix.<sup>35</sup> It is the amount of free water that is crucial for oxygen transport. The ratio of freezing to non-freezing water in the polymer influences the properties of hydrogels. Thus it is necessary to survey the freezing and non-freezing water contents of SIPNs in more detail to gain further understanding of the structure/property relationship.

It must be remembered that while the mechanical properties of SIPNs changed when the EBPU content was increased, the ratio of the hydrophilic component to THFMA also changed in each series of SIPNs. When the effect of the ratio of hydrophilic component to hydrophobic component on mechanical properties is considered, it is clear that the “transition” at 15.0% EBPU is caused largely by a change in the constituent monomer ratios. In general, as the EBPU content was increased a steady enhancement in the TS and TM had been observed.

Based on a previous study,<sup>37</sup> the optimum range of concentration of EBPU used in SIPNs was between 10.0% and 22.0% (by weight). If the concentration of the EBPU was lower than 10.0%, there was no contribution to enhancement of the hydrogel mechanical properties to an appreciable extent. If the concentration was higher than 22.0%, the EBPU did not dissolve in the monomer solutions completely.

Although water structure plays an important part in controlling the permeation properties of hydrogels, the usefulness of this characteristic is, in many cases, compromised by undesirable changes in mechanical strength. The TM of the material indicates the stiffness of the material. When the hydrophilic monomer content of the hydrogel is increased, a consequential decrease in stiffness is expected due to a higher percentage of plasticising FWC. Thus, when EWC was increased, the TS, TM of the SIPNs and MMA-based copolymers had decreased (Tables I and II, respectively), this

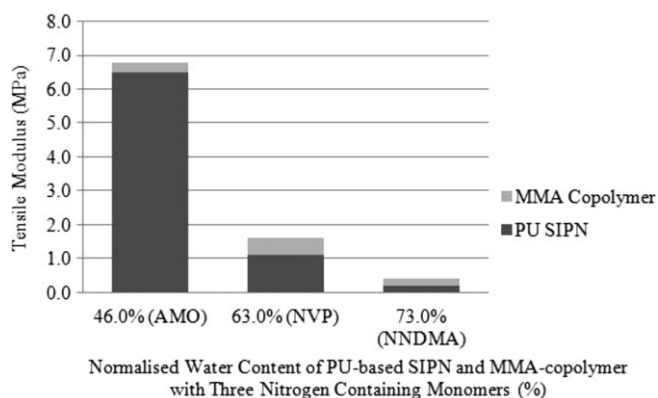


**FIGURE 3.** Stacked bar chart showing comparison of tensile moduli for 10% PU-based SIPNs based on three nitrogen containing monomers and their equivalent MMA non-PU containing copolymers. (Data derived from Tables I and II – error bars not shown for ease of visual presentation). [AMO; acryloylmorpholine, MMA; methyl methacrylate, NNDMA; *N,N*-dimethylacrylamide, NVP; *N*-vinyl pyrrolidone, PU; ester-based polyurethane, SIPN; semi-interpenetrating network].

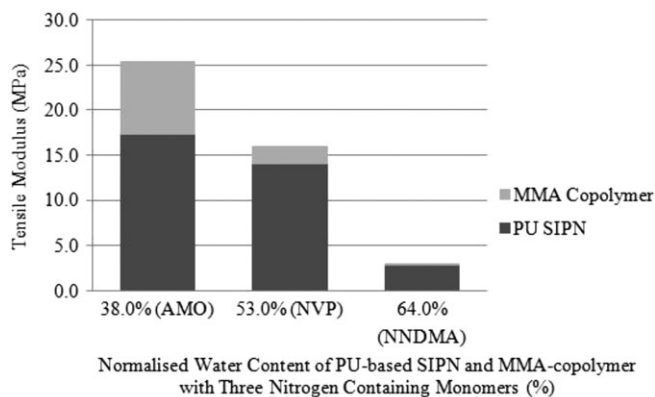


**FIGURE 4.** Stacked bar chart showing comparison of tensile moduli for 20% PU-based SIPNs based on three nitrogen containing monomers and their equivalent MMA non- PU containing copolymers. (Data derived from Tables I and II – error bars not shown for ease of visual presentation). [AMO; acryloylmorpholine, MMA; methyl methacrylate, NNDMA; *N,N*-dimethylacrylamide, NVP; *N*-vinyl pyrrolidone, PU; ester-based polyurethane, SIPN; semi-interpenetrating network].

characteristic change in properties had also been observed with 2-hydroxyethyl methacrylate (HEMA), HEMA-MMA copolymers reported by Barnes et al.<sup>40</sup>

For the SIPN materials and their equivalent simple MMA-based copolymers of similar water content, the former displayed higher TM than the latter (Figs. 3 and 4). Inclusion of the EBPU as the interpenetrant amplified the TM and TS of the SIPN materials but decreased the ETB in comparison to the MMA-based copolymers. The reinforcement provided by the EBPU to the polymer network, in particular the AMO and NVP-based SIPNs, highlights the fact that these materials are in the same TM range as corneal tissue stated earlier. Although EWC of the AMO SIPNs seldom increased higher than 48.1% (Table I), which is comparatively lower than the EWC of the cornea, both the AMO-based and NVP-based SIPN materials can be successful candidates for a KPro application.

Another important aspect of any synthetic material for a KPro application is its long term stability in a hydrated environment. Hydrolytic degradation over a prolonged period can lead to a reduction in the length of the EBPU-interpenetrant chains that reinforce the polymer network, which can result in material-failure of the prosthesis and a need for removal by the surgeon. Note that all of the SIPN-based hydrogels described in Table I have been stored in distilled water at room temperature for a period of 10 years; simple tensile tests of the same hydrogel sheets had established there is no degradation in their mechanical properties.

It is of interest to note that clear NNDMA-PMMA SIPN materials had been synthesized by Corkhill and Tighe<sup>32</sup> with an average EWC in excess of 85.0%. Additionally NNDMA-based SIPNs with cellulose acetate (CA) and cellulose acetate butyrate (CAB) used as interpenetrants, had also been reported with achievable EWC > 83.0%.<sup>31</sup> The EWC of NNDMA-based SIPNs presented in Table I are less than these reported values, however a larger selection of optically clear

materials were synthesized with the EBPU (10.0–21.8% monomer ratio) compared to when PMMA ( $\leq 5.0\%$  monomer ratio), CA ( $\leq 5.0\%$  monomer ratio) and CAB (2.0% monomer ratio) are used as interpenetrants with higher achievable TM values.

The proposed SIPN-based hydrogel materials for ophthalmic applications must be biotolerant. Several studies had suggested that the surface free energy of a hydrogel is an important property in determining the biotolerance of the material.<sup>41–43</sup> The surface properties of SIPNs were measured in dehydrated and hydrated states. The results are presented in Table I.

The measured surface free energy of a dehydrated polymer surface is a function of interactions that take place both at the surface and in the bulk of the polymer. The orientation of chemical functional groups at the polymer surface, which may be affected by the nature of the adjacent phase, influences the values obtained for the surface free energy.

Table I shows no evidence of any progressive contribution of EBPU to surface energies of the dehydrated membrane for the three series of SIPNs. When the EBPU content was increased, total surface free energy ( $\gamma^t$ ), the polar component ( $\gamma^p$ ), and dispersive component ( $\gamma^d$ ) of surface free energy changed slightly. However, it appears that the EBPU content did not greatly influence these values. The phenomenon can be explained by the fact that the polymeric “surfactant” (polyurethane) cannot easily diffuse through the dehydrated polymer.

In the dehydrated state, the SIPNs showed lower  $\gamma^p$  but higher  $\gamma^d$  values of surface free energy (Table I). This observation is consistent with the effect of the hydrophobic groups being expressed at the air interface and the orientation of the hydrophilic groups toward the polymer bulk. The surface of the polymer is therefore dominated by the hydrophobic groups and the value of the surface energy is dominated by the  $\gamma^d$ .

Any ophthalmic-based device in use exists in a hydrated environment, therefore any surface interaction between biological fluids and the prosthesis is influenced in the majority by  $\gamma^p$ . In this respect, the  $\gamma^d$  and  $\gamma^t$  of the hydrated SIPN-based hydrogels is not considered in Table I.

Surface groups rotate more freely in hydrated hydrogels compared to their dehydrated equivalents. An increase in polar moieties, subjugated by a higher hydrophilic monomer content, drives the increase in surface free energy (Table I). Despite the fact that use of multiple monomers in composition (AMO, NVP, NNDMA, and THFMA) may restrict the freedom of rotation around the backbone of the polymer, because of their ring or  $\alpha$ -methyl group structures. Thus in the hydrated state it appears that the surface of the materials remain dominated by the hydrophilic groups at the surface.

Use of water immersion (captive air bubble and octane droplet) techniques maintains the hydrogel surface in a hydrated state, but makes it difficult for the inverted droplet probes to displace the adsorbed water layers. For this reason the results were modified by the water layer. In other studies on adsorbed species on polymer surfaces, it was

demonstrated that the values of the surface energy components of such systems are a function of both adsorbed and substrate layers.<sup>44</sup> The deformation of the air bubble or octane droplet also led to variations in values obtained for similar materials. Therefore, this technique was useful to make comparisons between materials where trends may be observed, but actual values for contact angles among operators can be significantly varied.

A comparison of the dehydrated  $\gamma^t$  and hydrated  $\gamma^p$  values for all three families of SIPN-based materials is presented in Figure 5. If an average is taken for  $\gamma^t$  (43.0 mN m<sup>-1</sup>) and  $\gamma^p$  (27.0 mN m<sup>-1</sup>), these values were comparatively lower than equivalent average surface free energy measurements for clear NNDMA-PMMA SIPN materials reported at 49.0 mN m<sup>-1</sup> and 37.0 mN m<sup>-1</sup>, respectively<sup>32</sup>. Another similarity is observed if an average measurement is taken for dehydrated  $\gamma^t$  and hydrated  $\gamma^p$ , the values can be approximated for clear SIPN derivatives of NNDMA-CA as 48.2 mN m<sup>-1</sup>, 36.7 mN m<sup>-1</sup> and absolutely for NNDMA-CAB as 52.1 mN m<sup>-1</sup>, 36.6 mN m<sup>-1</sup>, respectively.<sup>31</sup>

In the hydrated state the EBPU appears to migrate to the surface and the polar moieties are able to express themselves, independent of the hydrophobic interpenetrant content. When exposed to air during contact angle measurement, the hydrophobic groups dominate the surface and hydrophilic groups orientate inward toward the bulk of the polymer. Two factors which may result in a difference of surface free energies between the contribution of hydrophilic monomers and the hydrogel SIPNs with the EBPU are variations in monomer chain length and a reduced surface segregation of EBPU.

For biological fluids, such as blood and tears, the  $\gamma^p$  is approximately 22.0 mN m<sup>-145</sup>. As shown in Table I, the

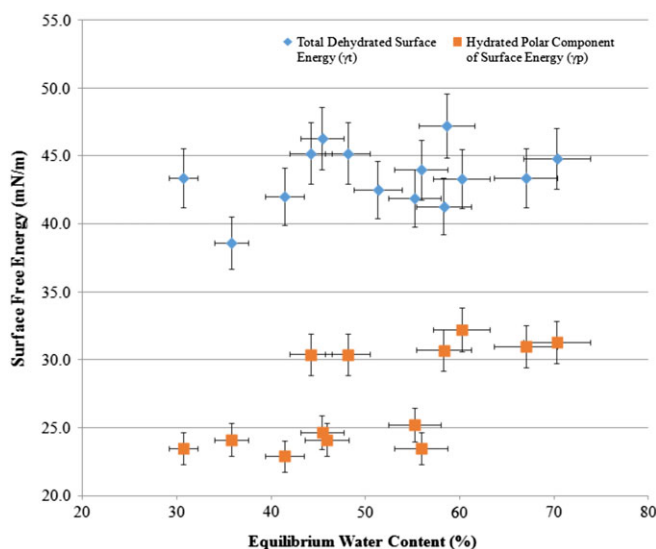


**FIGURE 5.** Scatter graph showing surface free energies of families of SIPN materials studied in their respective hydrated and dehydrated states (data from Table I). The x axis corresponds to the equilibrium water content of the hydrated materials. [ $\gamma^p$ ; polar component of surface free energy,  $\gamma^t$ ; total surface free energy, SIPN; semi-interpenetrating network].

majority of the hydrated SIPN materials with EBPU contents of 16.8% and higher possess  $\gamma^p$  values within the range of the  $\gamma^p$  values of biological fluids. If the  $\gamma^p$  is compared to that of pure water (51.0 mN m<sup>-1</sup>), the equivalent  $\gamma^p$  values for the SIPN materials are approximately half. The fact that the SIPN materials contain hydrophobic moieties from the EBPU interpenetrant and the hydrocarbon “segments” of the hydrophilic monomers inherently ensured lower  $\gamma^p$  values compared to that of pure water.

The results presented here confirm earlier observations<sup>31,32,39</sup> that inclusion of an interpenetrant in the form of a SIPN produces very similar water contents to those of the host hydrogel. As shown in Table I, it is the concentration of the hydrophilic monomers that drives the water content – as in the case with conventional hydrogel copolymers.<sup>46</sup>

Although the interpenetrant has little effect on the water content of the SIPN, once a critical concentration has been reached there is a marked effect of the interpenetrant on both surface and mechanical properties. Table I shows that once the interpenetrant concentration reaches about 10.0% the concentration is high enough to exert a significant effect on network deformation. This again is consistent with observations on hydrogel SIPNs based on different interpenetrant systems.<sup>39</sup> Although the crosslink concentration has a significant effect on the mechanical properties of conventional hydrogels<sup>46</sup> these effects are much smaller than those achieved with interpenetrant technology, and in these systems the concentration of the cross-linking agent EGDMA is maintained at 1.0% in the monomer mixture.

The effect of the interpenetrant on the surface properties of hydrogel copolymers is analogous to the effect of a surfactant. Because the interpenetrant chains are more hydrophobic than the hydrated hydrophilic monomer segments there is a thermodynamic drive to reach the air interface, restricted by polymer entrapment. The difference between the surface properties of the simple copolymer hydrogels and the hydrogel SIPNs, together with the concentration threshold for maximum effect of the interpenetrant (ca > 15.0%, Table I) support this model.

## CONCLUSIONS

These studies demonstrate that a range of optically clear SIPNs can be produced from combinations of acrylamido or amide-containing liquid monomers with EBPU interpenetrants. The compositional ranges that avoid phase separation are extensive and produce SIPNs that have a range of water contents (typically 30–60%) and enhanced (typically by factors of 10–100) tensile moduli compared to those of conventional MMA-based hydrogel copolymers of similar water content. Although the materials development was stimulated by ophthalmic applications they have potential applicability in other fields.

## REFERENCES

1. Bhamra TS, Tighe BJ. Mechanical properties of contact lenses: the contribution of measurement techniques and clinical feedback to 50 years of materials development. *Cont Lens Anterior Eye* 2017; 40(2):70–81.



2. Aloy MA, Aduara JE, Cerda-Duran P, Obergaulinger M, Esteve-Taboada JJ, Ferrer-Blasco T, Montes-Mico R. Estimation of the mechanical properties of the eye through the study of its vibrational modes. *Plos One* 2017;12(9):19.
3. Corkhill PH, Hamilton CJ, Tighe BJ. The design of hydrogels for medical applications. *Crit Rev Biocompat* 1990;5(4):363–436.
4. Liu J, Roberts CJ. Influence of corneal biomechanical properties on intraocular pressure measurement: quantitative analysis. *J Cataract Refr Surg* 2005;31(1):146–155.
5. Zhang Y, Li Y, Du Y, Shi Z, Cui Z. An overview of the material and structure of the porous scaffold for artificial cornea. *J Nanoeng Nanomanuf* 2014;4(4):279–288.
6. Salvador-Culla B, Kolovou PE. Keratoprosthesis: a review of recent advances in the field. *J Funct Biomater* 2016;7(2):13–23.
7. Myung D, Duhamel PE, Cochran JR, Noolandi J, Ta CN, Frank CW. Development of hydrogel-based keratoprotheses: a materials perspective. *Biotechnol Prog* 2008;24(3):735–741.
8. Biazar E, Ahmadian M, Heidari KS, Gazmeh A, Mohammadi SF, Lashay A, Heidari M, Eslami H, Sahebzalmani M, Hashemis H. Electro-spun polyethylene terephthalate (PET) mat as a keratoprosthesis skirt and its cellular study. *Fiber Polym* 2017;18(8):1545–1553.
9. Bakhshandeh H, Soleimani M, Hosseini SS, Hashemi H, Shabani I, Shafiee A, Nejad AHB, Erfan M, Dinarvand R, Atyabi F. Poly ( $\epsilon$ -caprolactone) nanofibrous ring surrounding a poly(vinyl alcohol) hydrogel for the development of a biocompatible two-part artificial cornea. *Int J Nanomed* 2011;6:1509–1515.
10. Cao D, Zhang Y, Cui Z, Du Y, Shi Z. New strategy for design and fabrication of polymer hydrogel with tunable porosity as artificial corneal skirt. *Mater Sci Eng C* 2017;70:665–672.
11. Klufas MA, Colby KA. The Boston Keratoprosthesis. *Int Ophthalmol Clin* 2010;50(3):161–175.
12. Saeed HN, Shanhag S, Chodosh J. The Boston keratoprosthesis. *Curr Opin Ophthalmol* 2017;28(4):390–396.
13. Zarei-Ghanavati M, Avadhanam V, Perez AV, Liu C. The osteo-odonto-keratoprosthesis. *Curr Opin Ophthalmol* 2017;28(4):397–402.
14. Tighe BJ. Rigid contact lenses. In: Efron N, editor. *Contact Lens Practice*. Oxford: Butterworth-Heinemann; 2010pp. 145–153.
15. Swarbrick HA. Orthokeratology review and update. *Clin Exp Optom* 2006;89(3):124–143.
16. Cheng HC, Liang JB, Lin WP, Wu R. Effectiveness and safety of overnight orthokeratology with Boston XO2 high-permeability lens material: a 24 week follow-up study. *Cont Lens Anterior Eye* 2016;39(1):67–71.
17. Haque S, Fonn D, Simpson T, Jones L. Corneal refractive therapy with different lens materials, part 1: corneal, stromal, and epithelial thickness changes. *Optometry Vision Sci* 2007;84(4):343–348.
18. Lu F, Simpson T, Sorbara L, Fonn D. Corneal refractive therapy with different lens materials, part 2: effect of oxygen transmissibility on corneal shape and optical characteristics. *Optometry Vision Sci* 2007;84(4):349–356.
19. van der Worp E, Bornman D, Ferreira DL, Faria-Ribeiro M, Garcia-Porta N, González-Meijome JM. Modern scleral contact lenses: a review. *Cont Lens Anterior Eye* 2014;37(4):240–250.
20. Fadel D. Modern scleral lenses: Mini versus large. *Cont Lens Anterior Eye* 2017;40(4):200–207.
21. Alipour F, Jabarvand Behrouz M, Samet B. Mini-scleral lenses in the visual rehabilitation of patients after penetrating keratoplasty and deep lamellar anterior keratoplasty. *Cont Lens Anterior Eye* 2015;38(1):54–58.
22. Severinsky B, Wajnsztajn D, Frucht-Pery J. Silicone hydrogel mini-scleral contact lenses in early stage after corneal collagen cross-linking for keratoconus: a retrospective case series. *Clin Exp Optom* 2013;96(6):542–546.
23. O'Donnell C, Maldonado-Codina C. A hyper-Dk piggyback contact lens system for keratoconus. *Eye Contact Lens* 2004;30(1):44–48.
24. Romero-Jiménez M, Santodomingo-Rubido J, Wolffsohn JS. Keratoconus: a review. *Cont Lens Anterior Eye* 2010;33(4):157–166.
25. Tighe BJ. Contact lens materials. In: Phillips AJ, Speedwell L, editors. *Contact Lenses*. Oxford: Butterworth-Heinemann; 1997pp. 50–63.
26. Tighe BJ. The design of polymers for contact lens applications. *Br Polym J* 1976;8(3):71–77.
27. Dragan ES. Design and applications of interpenetrating polymer network hydrogels. A review. *Chem Eng J*. 2014;243:572–590.
28. Rao CRK, Narayan R, Raju KVS. Interpenetrating and semi-interpenetrating polymer networks of polyurethane. In: Thomas S, Grande D, Cvelbar U, Raju KVS, Narayan R, Thomas S, editors. *H AMicro- and Nano-Structured Interpenetrating Polymer Networks : From Design to Applications*. New Jersey, USA: John Wiley & Sons Inc; 2016 pp. 259–282.
29. Lelah MD, Cooper SL, editors. *Polyurethanes in Medicine*. Boca Raton, FL: CRC Press; 1986.
30. Hartmann L, Watanabe K, Zheng LL, Kim CY, Beck SE, Huie P, Noolandi J, Cochran JR, Ta CN, Frank CW. Toward the development of an artificial cornea: improved stability of interpenetrating polymer networks. *J Biomed Mater Res B* 2011;98B(1):8–17.
31. Corkhill PH, Tighe BJ. Synthetic hydrogels: 7. High EWC semi-interpenetrating polymer networks based on cellulose esters and N-containing hydrophilic monomers. *Polymer* 1990;31(8):1526–1537.
32. Corkhill PH, Tighe BJ. Synthetic hydrogels. Part 8.-physicochemical properties of N,N-dimethylacrylamide semi-interpenetrating polymer network hydrogels. *J Mater Chem* 1992;2(5):491–496.
33. Yocum RH, Nyquist EB, editors. *Functional Monomers, Vol 1 & 2*. New York: Marcel Dekker; 1973.
34. Pedley DG, Tighe BJ. Water binding-properties of hydrogel polymers for reverse-osmosis and related applications. *Br Polym J* 1979;11(3):130–136.
35. Corkhill PH, Jolly AM, Ng CO, Tighe BJ. Synthetic hydrogels .1. Hydroxyalkyl acrylate and methacrylate copolymers – water binding-studies. *Polymer* 1987;28(10):1758–1766.
36. Murphy S, Hamilton CJ, Tighe BJ. Synthetic hydrogels: 5. Transport processes in 2-hydroxyethyl methacrylate copolymers. *Polymer* 1988;29(10):1887–1893.
37. Corkhill PH. *Novel hydrogel Polymer PhD Thesis*. Birmingham: Aston University; 1988.
38. Middleton I. *Acrylamide-based hydrogels for continuous Wear Contact lenses*. PhD Thesis. Birmingham: Aston University; 1981.
39. Corkhill P, Fitton J, Tighe B. Towards a synthetic articular cartilage. *J Biomater Sci Polym Ed* 1993;4(6):615–630.
40. Barnes A, Corkhill PH, Tighe BJ. Synthetic hydrogels: 3. Hydroxyalkyl acrylate and methacrylate copolymers: surface and mechanical properties. *Polymer* 1988;29(12):2191–2202.
41. Baier RE, Dutton RC, Gott VL. *Surface Chemical Features of Blood Vessels Walls and of Synthetic Materials Exhibiting Thromboresistance*. *Advances in Experimental Medicine, Surface Chemistry of Biological Surface*. New York: Plenum Press; 1970pp. 235–260.
42. Andrade JD. *Interfacial phenomena and biomaterials*. *Med Instrum* 1973;7:110–120.
43. Coleman DL, Gregonis DE, Andrade JD. Blood-materials interactions: the minimum interfacial free energy and the optimum polar/apolar ratio hypotheses. *J Biomed Mater Res* 1982;16(4):381–398.
44. Clay CS, Lydon MJ, Tighe BJ. *Biomaterials and Clinical Applications*. In: Pizzoferrato A, Marchetti PG, Ravaglioli A, Lee AJC, editors. Amsterdam: Elsevier Science; 1987.
45. Bright A, Tighe BJ. The composition and interfacial properties of tears, tear substitutes and tear models. *J Br Contact Lens Ass* 1993;16:57–66.
46. Tighe BJ, Mann A. 4 - physicochemical properties of hydrogels for use in ophthalmology. In: Chirila TV, Harkin DG, editors. *Biomaterials and Regenerative Medicine in Ophthalmology*, 2nd ed. Cambridge, UK: Woodhead Publishing; 2016pp. 75–100.